Atmospheric Turbulence and Fog Attenuation Effects in Controlled Environment FSO Communication Links

Abdullah Nafis Khan, Saad Saeed, Yasir Naeem, Muhammad Zubair, *Senior Member, IEEE*, Yehia Massoud, *Fellow, IEEE*, and Usman Younis, *Senior Member, IEEE*

***Abstract*— Free-space optical (FSO) communication can be seen as a promising technology for point-to-point and back-hauling links in the next generation wireless networks (5G and beyond) where cell size may shrink to a few hundred meters. In this work, we have experimentally investigated the laser beam propagation for FSO link under atmospheric turbulence and fog conditions. A controlled atmospheric environment chamber is designed to perform experiments under varying channel conditions. For fog attenuation, we have proposed an empirical model as a function of visibility against the measured average values, for visibility range of $0 \leq V \leq 1000$ m. For atmospheric turbulence, we report the measured values of the refractive index structure parameter C_n^2. The measured C_n^2 is used to calculate the atmospheric coherence width along the propagation distance. This work would help in the design optimization of practical FSO links under adverse conditions like fog and atmospheric turbulence.**

***Index Terms*— Optical attenuation, atmospheric turbulence, free space optics.**

I. Introduction

FREE space optical communication (FSO) has been used to solve the inherent last mile bottleneck of wireless and wired networks, especially in dense urban areas by offering unlimited bandwidth in unlicensed spectrum, and by achieving a cost effective and reliable communication system. The FSO communication can be used as fault protection backhauling to the existing optical fiber communication system, therefore improving the overall network performance by reducing the network downtime [1]. Moreover, FSO transmission channels can be used to provide rapid connectivity to the geographical constrained areas for sensor network applications [2]. The propagating optical wavelength undergoes effects like scattering and absorption in random atmospheric weather conditions such as fog, rain, snow, and dust. The atmospheric turbulence effect, which causes the refractive index of air to vary due to the existence of thermal gradients from sunlight heating, causes the optical beam to experience intensity fluctuations even in clear weather. The measure of refractive index structure parameter C_n^2 is critical to explain the turbulence strength. In [3], C_n^2 is expressed in terms of fractional-dimension parameter D to optimize the input beam parameters of the FSO communication system to enhance link reliability. Similarly in [4], an optimization problem has been developed to study the FSO link performance under saturation regime to mitigate the effects of pointing errors and atmospheric turbulence. Moreover, C_n^2 dependence has been studied for vertical profiles of atmospheric aerosols distribution [5]. Because it is difficult to repeat measurements under identical conditions and to predict the occurrence of specific atmospheric effects like fog, rain, smoke, and dust events, the authors in [6], [7], and [8] conducted a ground-breaking but preliminary investigation of the FSO performance using controlled environments (chamber) and proposed empirical models that are close to the specific environment condition. In [9], the study shows that 10 μm in Far-Infrared (FIR) has higher transmission through fog, however high cost hardware will be required, which is not readily available. Therefore, almost all commercially available FSO links operate in the visible and near-Infrared spectrum range. Consequently, for this study we have selected wavelength from the visible spectrum to analyse the dependence on fog in a controlled atmospheric chamber environment. The motivation behind this wavelength selection was the low cost and availability of hardware needed to design a basic FSO communication link. These effects are significant enough to cause performance degradation and link availability of the FSO communication system. As a result, one of the key subjects to characterise the FSO link availability is the investigation of the relationship between various wavelengths and atmospheric conditions.

In this work, we report real-time measurements for optical beam propagating through atmospheric conditions of fog in a controlled atmospheric chamber, along with measured values of visibility, and proposed an empirical attenuation model for wavelength of 633 nm based upon the measurements. We also

Manuscript received 19 September 2022; revised 13 October 2022; accepted 19 October 2022. Date of publication 28 October 2022; date of current version 8 November 2022. This work was supported in part by the Higher Education Commission (HEC) through National Research Program for Universities (NRPU) under Grant 10136. The work of Muhammad Zubair was supported by Innovative Technologies Laboratories (ITL), King Abdullah University of Science and Technology (KAUST). *(Corresponding authors: Muhammad Zubair; Usman Younis; Yehia Massoud.)*

Abdullah Nafis Khan, Saad Saeed, Yasir Naeem, and Usman Younis are with the Department of Electrical Engineering, Information Technology University of the Punjab, Lahore 54600, Pakistan (e-mail: usman.younis@itu.edu.pk).

Muhammad Zubair is with the Department of Electrical Engineering, Information Technology University of the Punjab, Lahore 54600, Pakistan, and also with Innovative Technologies Laboratories (ITL), King Abdullah University of Science and Technology (KAUST), Thuwal 23955, Saudi Arabia (e-mail: muhammad.zubair@itu.edu.pk).

Yehia Massoud is with Innovative Technologies Laboratories (ITL), King Abdullah University of Science and Technology (KAUST), Thuwal 23955, Saudi Arabia (e-mail: yehia.massoud@kaust.edu.sa).

Color versions of one or more figures in this letter are available at https://doi.org/10.1109/LPT.2022.3217072.

Digital Object Identifier 10.1109/LPT.2022.3217072

TABLE I
VISIBILITY RANGE FOR DIFFERENT FOG CONDITIONS

Fog Type	Light	Moderate	Thick	Dense
Visibility (m)	500∼1000	200∼500	50∼200	0∼50

report the measured values of the refractive index structure parameter (C_n^2), which defines the strength of atmospheric turbulence. Moreover, the Fried parameter against the temperature gradient has been calculated for measured values of C_n^2. This work can be of help to FSO operators to engineer the link for maximum uptime with optimized values of laser power.

The rest of the letter is organised as follows. Characterization of fog and visibility, along with atmospheric chamber design is discussed in Section II. The measured results are presented in Section III. Finally the work is concluded in Section IV.

II. EXPERIMENTAL SETUP DESIGN

A. Characterization of Fog and Visibility

In FSO communication link, the operating wavelength is selected from the low absorption band of spectrum. Therefore, propagating laser beam is more affected by atmospheric scattering compared to absorption. The optical signal is scattered by the atmospheric particles that have a size which is comparable to wavelength. Among various weather conditions fog turns out to be the worst as the signal attention can be high enough for FSO link outage. Fog is composed of fine water droplets suspended in air that can reduce the visibility. According to meteorological definition, fog occurs when the visibility drops to nearly 1 km [8]. The link visibility is used to characterise the intensity of fog. Visibility is the distance at which the visual contrast of an object drops to 2% of the original visual contrast of that object based on the Koschmieder law. The 2% drop is known as the threshold T_{th} for the atmospheric propagation path, based upon which the meteorological visibility V can be defined in terms of α and T_{th} as follows [8]:

$$V = -\frac{10\log_{10} T_{th}}{\alpha}, \quad \text{(km)} \tag{1}$$

where $T_{th} = 0.02$. The signal attenuation (α) is given as follows [8]:

$$\alpha = -\frac{10\log_{10} T}{4.343L}, \quad \text{(dB/km)} \tag{2}$$

where L is the propagation link distance and T is the transmittance of optical signal at 550 nm. The transmittance T is computed as the ratio of received optical power when their is fog to that when there is no fog. The visibility range defines the fog event in four different categories, presented in Table I.

B. Atmospheric Chamber Design

The atmospheric channel is random in nature therefore it is difficult to perform experiments under a typical weather condition to study the behavior of laser beam propagation. However, the atmospheric chambers are designed to emulate the real-time specific atmospheric condition to study the effects on laser beam propagation. In figure 1, a chamber of $100\times38\times$

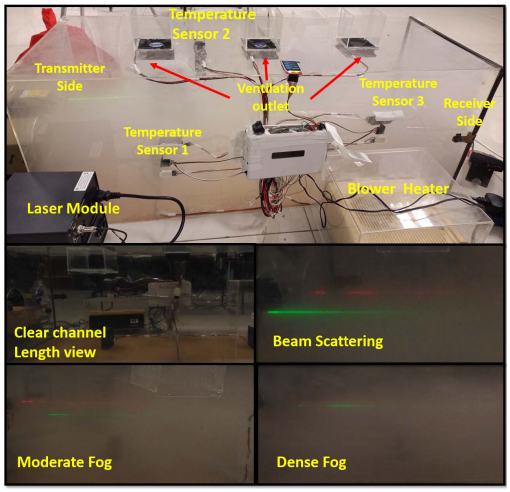

Fig. 1. Experimental setup of atmospheric chamber used to measure optical attenuation and C_n^2. The inset below shows different atmospheric conditions including clear, moderate, and dense fog scenarios. Beam scattering can be seen due to the presence of fog inside the chamber.

38 cm^3 dimension, used to create the effect of the atmospheric channel is shown. The chamber is equipped with a humidifier machine (HF-507) which generates the fog. The fans within the chamber are used to distribute the fog within the chamber to create a homogeneous channel environment. Temperature sensors (DHT-22), having a measuring accuracy of ±0.5°C, are placed inside the chamber with a separation distance of 50 cm at three different locations. A pressure sensor (BMP-388) with measuring accuracy of ±0.5 millibar is placed inside the chamber to measure the atmospheric pressure. All the sensors are connected to a microcontroller (Arduino Mega 2560) for the purpose of real-time data acquisition. We used a CNI laser module (MRL-III-633F) from the visible spectrum of wavelength 633 nm, at the transmitter, operating at 4 mW. The transmitted optical signal propagates along the channel, before being collected at the silicon-photodiode of the receiver power meter (UT385). To measure the link visibility, a CNI laser module (MGL-III-532) of wavelength 532 nm was used simultaneously, operating at 2 mW. The measured values along with equations (1) and (2) are used to calculate the visibility of the foggy channel.

The chamber was filled with fog until the received optical power of the laser beam reached its minimum value, which was observed for 30 seconds, before the data acquisition process started and the received optical power was automatically measured at an interval of 0.1 sec. The fog particles gradually escape through the small outlets along the chamber and the data acquisition lasts until the optical power returns to its initial value, same as at the transmitter. The data was collected for 10 repetitions. All the experimental measurements were carried out in a dark room, to avoid background noise. Different fog conditions can be seen in figure 1. Similarly, to measure the refractive index structure parameter (C_n^2), the pressure is kept constant and a temperature gradient is introduced within the chamber, in which the air intake at one end is kept at room temperature and the hot air is blown inside the chamber from the opposite end using an electrical

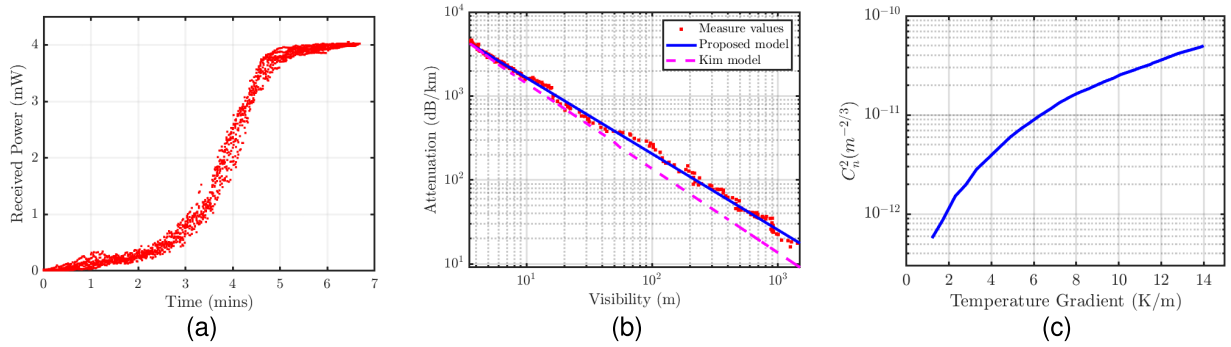

Fig. 2. (a) Measured signal strength for variable fog conditions inside the atmospheric chamber. (b) Optical attenuation against visibility is plotted for average measured values of optical signal along with the proposed empirical model and Kim model. (c) Measured average values of refractive index structure parameter C_n^2 against temperature gradient under controlled atmospheric chamber environment.

heater. The data acquisition process for all temperature sensors starts once the heater blower turns on.

III. Results and Discussion

A. Optical Signal Attenuation

Figure 2(a) shows the received signal power against time. The measured power values depict low divergence for all the repetitions, hence demonstrating the capability of experimental setup, producing same results under controlled environment. In figure 2(b), we calculated the optical attenuation versus visibility for 633 nm. For dense fog conditions with extremely low visibility ($0 \leq V \leq 50$ m), the attenuation exceeds over 400 dB/km. The average attenuation for thick fog with visibility range of ($50 \leq V \leq 200$ m) varies in between 400 dB/km to 112 dB/km. Similarly, for moderate fog conditions ($200 \leq V \leq 500$ m), the corresponding attenuation ranges from 112 dB/km to 45 dB/km. The optical attenuation substantially decreases for light fog condition, and is measured as 23 dB/km for visibility at 1000 m. The average measured values are in good agreement with the proposed fog model in [8], for visibility range ($0 \leq V \leq 200$ m).

The attenuation and visibility have a reciprocal relationship seen from the plot in figure 2(b). Based on the average measured data, we proposed an optical attenuation model as a function of visibility for 633 nm under atmospheric conditions of fog. Using the Matlab non-linear least square technique we proposed a power law fit expressed as [7]:

$$\alpha = b \times V^{-a}, \quad \text{(dB/km)} \tag{3}$$

given, V is the visibility in km, a and b are the power law coefficients with values of $a = 0.9063$ and $b = 25.36$. The proposed model fits well with the average measured data. To measure the accuracy of the of proposed model the R-square value was found to be 0.99, whereas the parameters confidence bound for 95% certainty is found to be: $a = 0.9063$ (0.9085, 0.9042) and $b = 25.36$ (25.07, 25.65), with both intervals laying within a narrow limit, hence showing precise estimation of coefficients. The value for root mean square error (RMSE) between the proposed model and the measure data is found to be 12.08 dB for the range of visibility as given in figure 2(b).

Figure 2(b) shows the comparison between the proposed model (3) with the Kim Model for fog attenuation. The Kim model is expressed as [9]:

$$\alpha = \frac{17}{V}\left(\frac{0.550}{\lambda}\right)^{-q}, \quad \text{(dB/km)} \tag{4}$$

where, V is the visibility (km) and λ is the optical wavelength in the visible range ($400 \leq \lambda \leq 700$ nm). The q is the scattering particle size distribution classified as:

$$q = \begin{cases} 1.6, & V > 50 \text{ km} \\ 1.3, & 6 \text{ km} < V < 50 \text{ km} \\ 0.16V + 0.34, & 1 \text{ km} < V < 6 \text{ km} \\ V - 0.5, & 0.5 \text{ km} < V < 1 \text{ km} \\ 0. & V < 0.5 \text{ km} \end{cases}$$

The proposed model shows good agreement with the average measured data, as well as with the Kim's model at $\lambda = 633$ nm for the visibility range ($0 \leq V \leq 100$ m). However, the values of the proposed model attenuates approximately ~1.5 times more compared to Kim's model, for visibility range ($100 \leq V \leq 1000$ m). It can be said that the optical signal attenuates more in the atmospheric chamber environment compared to outdoor channel conditions. Even so, this can aid in modelling and designing effective FSO links for reliable communication.

B. Refractive Index Structure Parameter

A very useful and widely used parameter to express the strength of atmospheric turbulence is called refractive index structure parameter C_n^2, and is given as [10]:

$$C_n^2 = \left(79 \times 10^{-6}\frac{P}{T^2}\right)^2 C_T^2, \quad (\text{m}^{-2/3}) \tag{5}$$

where, P = 970 millibar is the atmospheric pressure and T is the temperature in Kelvin scale. The C_T^2 is the temperature structure parameter for statistically homogeneous and isotropic fluctuations and is given as:

$$C_T^2 = \sqrt{\langle \partial T^2 \rangle r^{-1/3}} \tag{6}$$

where, $\partial T = (T_1 - T_2)$, T_1 and T_2 are the temperatures at two arbitrary locations separated by distance $r = 50$ cm. The wavelength dependence is insignificant and are usually neglected [11]. The pressure fluctuations are altitude dependent therefore it remained constant for no change in height,

TABLE II
AVERAGE MEASURED VALUES OF TEMPERATURE AT FIVE DIFFERENT INSTANCES

No.	T1 (°C)	T2 (°C)	T3 (°C)	$C_n^2(m^{-2/3})$
1	26.1	27.8	30.5	4.77×10^{-12}
2	26.5	29.2	34.3	1.56×10^{-11}
3	26.9	30.6	36.6	2.33×10^{-11}
4	27.5	31.9	39.1	3.33×10^{-11}
5	28.2	32.8	42	4.95×10^{-11}

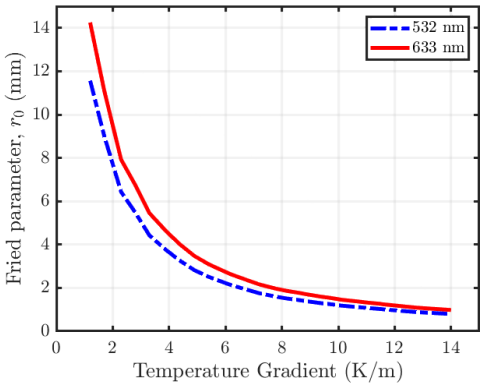

Fig. 3. Fried parameter or the atmospheric coherence length against the measured temperature gradient for two different wavelengths.

as considered in this work. Using equation (5) the turbulence strength can be determined for a varying temperature range of 25-42 $^{\circ}C$. Figure 2(c) shows the variations in C_n^2 against temperature gradient ($\Delta T/\Delta L$) and it can be deduced that for higher temperature gradient the turbulence strength increases, therefore the propagating laser beam can experience intensity fluctuations. Table II shows the average measured values of temperature sensors at five different instances, along with an average value of C_n^2 for the path length of 1 m. These average measured values of C_n^2 agree well with the reported values in [10] and [12].

C. Fried Parameter

The measured values of C_n^2 can be used to calculate system performance parameters such as the Fried parameter to corroborate our results. The Fried parameter is the function of C_n^2 and distance which describes the atmospheric coherence width, r_0, and is expressed as [11]:

$$r_0 = \left(0.432 \int_0^H C_n^2(h)dh \times k^2 sec(\theta)\right)^{-3/5} \quad (7)$$

where $k = 2\pi/\lambda$, h is the height, and $\theta = 0$ degree is the zenith angle. Figure 3 shows the variations in Fried parameter for the temperature gradient within the atmospheric chamber for wavelengths of 532 nm and 633 nm. The results show that the value of r_0 decreases as the temperature gradient increases corresponding to increase in atmospheric turbulence strength. It also shows that the r_0 increases for 633 nm compared to 532 nm, however the overall trend remains the same. Moreover, for given temperature gradients higher wavelengths (e.g 850 nm, 1300 nm and 1550 nm) can perform better, as the value of r_0 increases. It can be concluded that the received signal intensity decreases with the increase in turbulence strength.

The performance of FSO communication link is degraded due to low atmospheric coherence width. Under strong conditions, a link of a few hundred meters can be installed. In next generation networks (5G), cell size has shrunk to a few hundred meters, therefore with limited range in adverse atmospheric conditions, FSO can be seen as a promising low cost solution for point-to-point and back-hauling links [13].

IV. CONCLUSION

In this letter, we investigated the optical beam propagation for FSO communication link under a controlled atmospheric chamber environment and proposed attenuation model for specific wavelength of 633 nm under foggy conditions. The atmospheric chamber is used to measure the C_n^2 for varying temperature range from 25-42 $^{\circ}C$ for assorted temperature gradients. These results can be found helpful in estimating the practical values of refractive index structure parameter for geographical areas with high temperature gradients. The measured values of C_n^2 are used to calculate the atmospheric coherence width of the optical beam. Using the relationship present in [12], these chamber results of C_n^2 can be used to estimate the performance of outdoor FSO links. The chamber-experiments provides a basic framework for characterization of realistic free-space atmospheric channel before one can embark upon the long-distance field trials.

REFERENCES

[1] S. T. Hayle et al., "Integration of fiber and FSO network with fault-protection for optical access network," *Opt. Commun.*, vol. 484, Apr. 2021, Art. no. 126676.
[2] S. T. Hayle, Y. C. Manie, C.-K. Yao, T.-Y. Yeh, C.-H. Yu, and P.-C. Peng, "Hybrid of free space optics communication and sensor system using IWDM technique," *J. Lightw. Technol.*, vol. 40, no. 17, pp. 5862–5869, Sep. 1, 2022.
[3] A. N. Khan, U. Younis, M. Q. Mehmood, and M. Zubair, "Atmospheric propagation of space-fractional Gaussian-beam waves in a FSO communication system," *Opt. Exp.*, vol. 30, no. 2, pp. 1570–1583, 2022.
[4] M. A. Amirabadi and V. T. Vakili, "A new optimization problem in FSO communication system," *IEEE Commun. Lett.*, vol. 22, no. 7, pp. 1442–1445, Jul. 2018.
[5] K. Sunilkumar, N. Anand, S. Satheesh, K. K. Moorthy, and G. Ilavazhagan, "Enhanced optical pulse broadening in free-space optical links due to the radiative effects of atmospheric aerosols," *Opt. Exp.*, vol. 29, no. 2, pp. 865–876, 2021.
[6] Z. Ghassemlooy, J. Perez, and E. Leitgeb, "On the performance of FSO communications links under sandstorm conditions," in *Proc. 12th Int. Conf. Telecommun.*, 2013, pp. 53–58.
[7] M. A. Esmail, H. Fathallah, and M.-S. Alouini, "Outdoor FSO communications under fog: Attenuation modeling and performance evaluation," *IEEE Photon. J.*, vol. 8, no. 4, pp. 1–22, Aug. 2016.
[8] M. Ijaz, Z. Ghassemlooy, J. Pesek, O. Fiser, H. L. Minh, and E. Bentley, "Modeling of fog and smoke attenuation in free space optical communications link under controlled laboratory conditions," *J. Lightw. Technol.*, vol. 31, no. 11, pp. 1720–1726, Jun. 1, 2013.
[9] R. Nebuloni and E. Verdugo, "FSO path loss model based on the visibility," *IEEE Photon. J.*, vol. 14, no. 2, pp. 1–9, Apr. 2022.
[10] H. Kaushal et al., "Experimental study on beam wander under varying atmospheric turbulence conditions," *IEEE Photon. Technol. Lett.*, vol. 23, no. 22, pp. 1691–1693, Nov. 15, 2011.
[11] L. C. Andrews and R. L. Phillips, *Laser Beam Propagation Through Random Media*. Bellingham, DC, USA: SPIE, 2005.
[12] Z. Ghassemlooy, H. Le Minh, S. Rajbhandari, J. Perez, and M. Ijaz, "Performance analysis of Ethernet/Fast-Ethernet free space optical communications in a controlled weak turbulence condition," *J. Lightw. Technol.*, vol. 30, no. 13, pp. 2188–2194, Jul. 1, 2012.
[13] Y. Xu, G. Gui, H. Gacanin, and F. Adachi, "A survey on resource allocation for 5G heterogeneous networks: Current research, future trends, and challenges," *IEEE Commun. Surveys Tuts.*, vol. 23, no. 2, pp. 668–695, 2nd Quart., 2021.